UC Berkeley

UC Berkeley Previously Published Works

Title

Enhanced luminance of organic light-emitting diodes with metal nanoparticle electron injection layer

Permalink

https://escholarship.org/uc/item/0mv4q9t7

Journal

Applied Physics A: Materials Science & Processing, 96(2)

ISSN

1432-0630

Authors

Liu, Deang
Fina, Michael
Ren, Li
et al.

Publication Date

2009-08-01

DOI

10.1007/s00339-009-5199-x

Peer reviewed

eScholarship.org Powered by the California Digital Library
University of California

Appl Phys A (2009) 96: 353–356
DOI 10.1007/s00339-009-5199-x

Applied Physics A
Materials Science & Processing

Enhanced luminance of organic light-emitting diodes with metal nanoparticle electron injection layer

Deang Liu · Michael Fina · Li Ren · Samuel S. Mao

Received: 15 October 2008 / Accepted: 3 March 2009 / Published online: 2 April 2009
© The Author(s) 2009. This article is published with open access at Springerlink.com

Abstract Improvement of the performance of organic light-emitting diodes (OLEDs) was achieved by implementing Magnesium-Nickel nanoparticles at the cathode–organic interface using pulsed laser deposition technique. The small geometry of Mg-Ni nanoparticles acts to enhance the localized electric field around them, thus increasing electron injection through tunneling, from the cathode to the organic layer. Improved current and luminance characteristics were demonstrated for both small molecule and polymer-based OLEDs when the nanoparticle layer was incorporated.

PACS 68.35.bd · 78.60.Fi · 78.66.Qn · 85.60.Jb

1 Introduction

Organic light-emitting diodes (OLEDs) have attracted a tremendous interest due to their potential as energy-efficient solid-state lighting sources and for flat-panel display applications [1–6]. Although much of recent efforts have been devoted to the development of better semiconducting organic molecules as well as the optimization of OLED device performance, effective carrier injection especially at the cathode side of OLEDs remains a challenge [7–12]. One unique feature of OLEDs is that they are constructed with very thin organic layers (∼100 nm). From the manufacturing standpoint, thin film devices enable cost-effective and large scale fabrication on glass or flexible plastic substrates, for example. On the other hand, the very thin organic layers of OLEDs give rise to a large electric field between the two electrodes. Therefore, at the cathode–organic interface, field-assisted tunneling through an electronic energy barrier becomes an important charge injection mechanism [8].

In our previous work [13], imprinting microlithography technique was used to realize a structured cathode. The electric field at the cathode–organic interface was increased due to the resulting cathode geometry, which altered the otherwise flat equipotential planes near the cathode. According to the Fowler–Nordheim tunneling theory [14, 15], the current density at the cathode–organic interface depends strongly on local electric field: an increase in the field through micro- or nano-structuring would enable to enhance tunnel injection of electrons to cross the cathode–organic interface.

In the present study, we present a different approach to structuring the OLED cathode that has resulted in an improved device performance. Specifically, Magnesium-Nickel (Mg-Ni) nanoparticles were implemented at the cathode–organic interface using a pulsed laser deposition technique. The precursor target material for laser ablation and subsequent deposition was an Mg-Ni alloy target, in which Ni would help reduce the reactivity of the material due to the presence of elemental Mg. After Mg-Ni nanoparticles were incorporated, both the electron injection and the luminance characteristics of the OLEDs with different combinations of organic molecules and cathode materials were improved. Based on calculations of the electric field at the interface, we attributed the improvement of the device performance to enhanced electron tunnel injection to cross the cathode–organic interface due to the presence of Mg-Ni nanoparticles, which increased the local electric field intensity at the interface.

D. Liu · M. Fina · L. Ren · S.S. Mao (✉)
Lawrence Berkeley National Laboratory, University of California at Berkeley, Berkeley, CA 94720, USA
e-mail: ssmao@lbl.gov
Fax: +1-510-4867303

2 Experiments

Organic materials used for fabricating OLEDs in this study include Poly[2-methoxy-5-[(2′-ethylhexyl)oxy]-p-phenylenevinylene] (MEH-PPV, MW 150,000–250,000), N,N′-Di-[(1-naphthyl)-N,N′-diphenyl]-1,1′-biphenyl)-4,4′-diamine (NPB, 99%), 8-hydroxyquinoline aluminum (Alq_3, 99.995%) and Poly(3,4-ethylenedioxythiophene):poly(styrenesulfonate) (PEDOT:PSS, 2.8 wt% dispersion in H_2O), all acquired from Sigma-Aldrich Inc. Fabrication of OLEDs starts with cleaning ITO-coated glass substrates (200 nm, 20 Ω/□) using ultrasonic wave in acetone, alcohol and purified water. PEDOT:PSS was coated by spin casting and dried in a furnace at 150°C for 30 minutes. MEH-PPV films (approximately 100-nm-thick) were spin-coated from a chloroform solution. NPB and Alq_3 were thermally evaporated with a thickness of about 30 nm in a vacuum chamber under a pressure of $\sim 8 \times 10^{-7}$ Torr. Mg-Ni nanoparticles were deposited by pulsed laser deposition with a femtosecond Ti:Sapphire laser (wavelength 800 nm, pulse duration ~120 fs) ablating a prefabricated solid-state Mg-Ni target. LiF (0.8 nm) and other electrode materials, Ca (15 nm) and Al (50 nm), were also thermally evaporated in a vacuum environment ($\sim 8 \times 10^{-7}$ Torr). The current density–voltage characteristics of the OLEDs were measured with a Keithley source meter (model 2420). The luminance values were measured with a Minolta luminance meter (model LS-110). All the measurements were performed in a glovebox under nitrogen atmosphere.

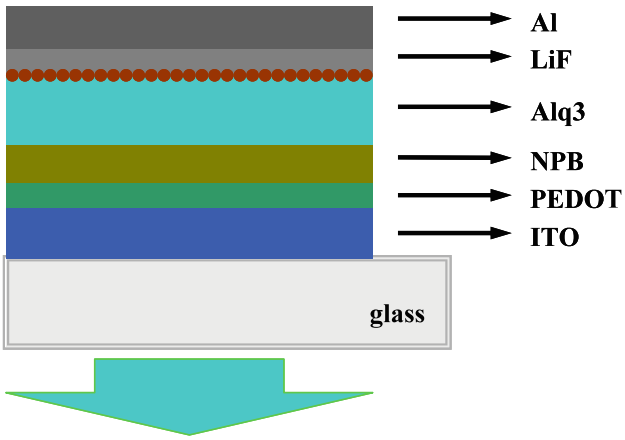

Fig. 1 Schematic illustration of an OLED device with incorporated nanoparticle layer at the cathode–organic interface

3 Results and discussions

Figure 1 is a schematic illustration of an OLED device with an incorporated nanoparticle layer at the cathode–organic interface. The device has the following structure, ITO/PEDOT:PSS/NPB/Alq_3/nanoparticles/LiF/Al. To understand the effect of the nanostructured cathode–organic interface on the local electric field, we calculated the field and compared it to that of a standard OLED with planar geometry. The Poisson equation governs the electric potential in the organic layers, and to simplify the analysis, we assumed that there is no unpaired charge so the equation can be simplified to the three-dimensional (3d) Laplace equation in rectangular coordinates,

$$\nabla^2\phi = \frac{\partial^2\phi}{\partial x^2} + \frac{\partial^2\phi}{\partial y^2} + \frac{\partial^2\phi}{\partial z^2} = 0, \quad (1)$$

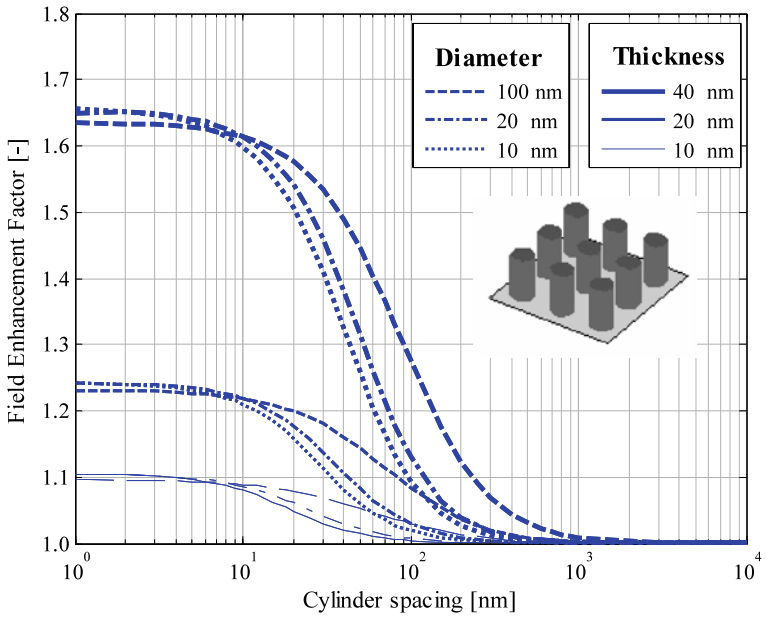

Fig. 2 Calculated electric field enhancement factor in an organic layer implemented with nanostructures of different geometry. The inset shows schematically an array of nanostructures used for the calculation

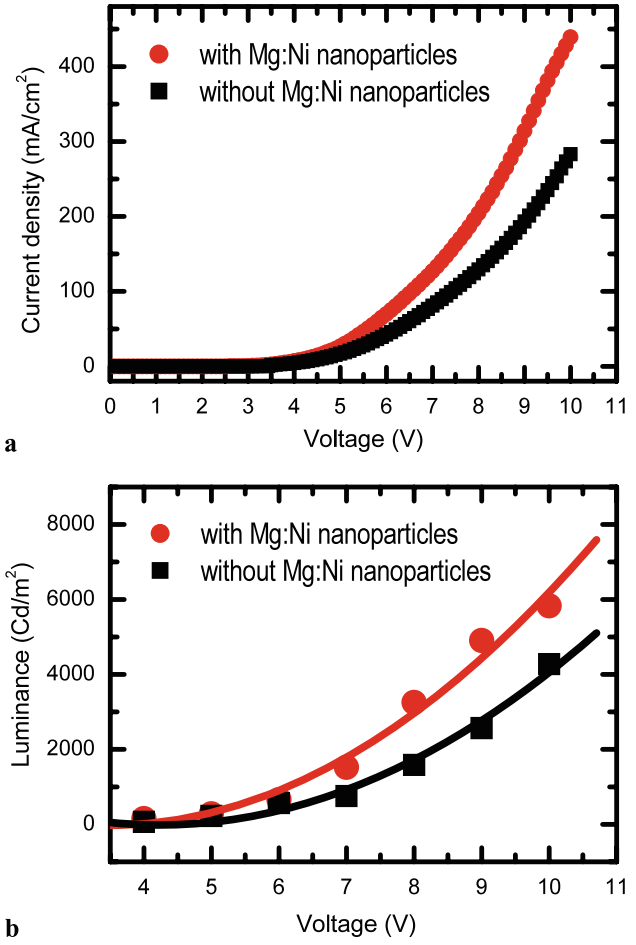

Fig. 3 (**a**) I–V and (**b**) L–V curves of small molecule-based OLED—Device A, ITO/PEDOT:PSS/NPB/Alq3/nanoparticles/LiF/Al. For comparison, the performance of a standard planar device without nanoparticles is also presented

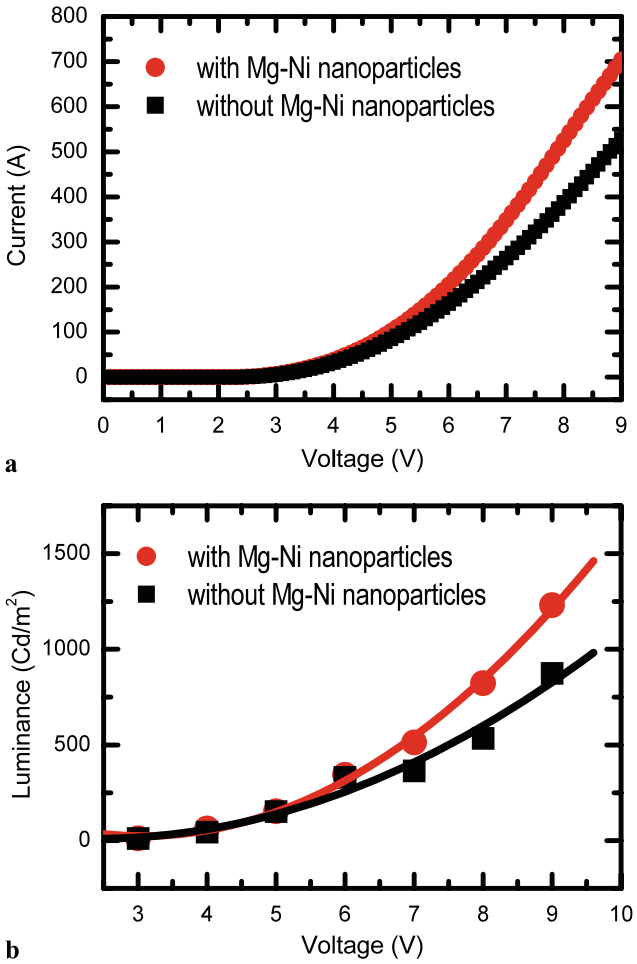

Fig. 4 (**a**) I–V and (**b**) L–V curves of polymer-based OLED—Device B, ITO/PEDOT:PSS/MEH-PPV/nanoparticles/Ca/Al. For comparison, the performance of a standard planar device without nanoparticles is also presented

where ϕ is the scalar electric potential. After obtaining the electric potential solution, the electric field along the cathode surface was determined. The following integration was performed to determine the overall electric field enhancement due to the structuring,

$$F_{3d} = \left(\sum_{\substack{\text{cathode} \\ \text{surfaces}}} \int_A E(x, y)\, dA \right) \Big/ (E_0 \cdot A_{\text{cathode}}), \tag{2}$$

where A_{cathode} is the area of the cathode in planar geometry, and E_0 represents the uniform electric field in OLEDs without a nanostructured cathode–organic interface. Figure 2 shows calculated field-enhancement factor, F_{3d}, resulting from the implementation of nanoscale cylinders of different geometry under an applied voltage of 10 V. The results suggest that a 20% increase in the electric field intensity should be achieved after incorporation of Mg-Ni nanoparticles with feature size of about 20 nm.

According to the Fowler–Nordheim tunneling theory [14, 15], the current density, J, resulted from electrons tunneling through a barrier, is related to the electric field, E, by the relation,

$$J \propto E^2 \exp\left(-\frac{a}{E}\right), \tag{3}$$

where a is a constant reflecting the property of the tunneling barrier. This equation shows that as the electric field is increased, current injection will increase significantly. By incorporating a layer of Mg-Ni nanoparticles that offers localized field enhancement due to the bending of otherwise flat equipotential planes, electron injection current density from the cathode would be increased as compared to the standard planar OLED devices.

Figure 3 shows the measured current density–voltage (I–V) curve and luminance–voltage (L–V) curve of a small molecule-based OLED (Device A) having the structure ITO/PEDOT:PSS/NPB/Alq_3/Mg-Ni nanoparticles/LiF/Al. Standard device without Mg-Ni nanoparticles was also fabricated and tested for comparison. The device with Mg-Ni

nanoparticles shows improved current density and luminance over the standard planar device. The turn-on voltage of the device with Mg-Ni nanoparticle incorporation was reduced. There was no apparent change of the emission spectra after Mg-Ni nanoparticles are implemented. Similarly to what we demonstrated in our previous work [13], the improved performance of the OLED devices can to be attributed to enhanced electron tunnel injection brought about by local field enhancement resulting from the small geometry of Mg-Ni nanoparticles.

We also implemented a nanoparticle layer between the cathode and organic layer in a polymer-based OLED. Device B has the structure ITO/PEDOT:PSS/MEH-PPV/Mg-Ni nanoparticles/Ca/Al. Figure 4 shows the measured I–V curve and L–V curve of Device B, which exhibits a similar performance improvement in both current density and luminance when the Mg-Ni nanoparticle layer was incorporated. Since the work function of Ca (2.9 eV) is lower than that of Mg (3.6 eV), the improvement cannot be attributed to the work function of Mg; instead, the small geometry of Mg-Ni nanoparticles has to be at the origin.

4 Conclusions

In summary, OLEDs with Mg-Ni nanoparticles implemented at the cathode–organic interface exhibit improved electron injection and luminance characteristics. The small geometry of Mg-Ni nanoparticles increases the local electric field at the interface, enhancing electron tunnel injection through the energy barrier. It was shown that the approach of incorporating Mg-Ni nanoparticles works well for both small molecule and polymer-based OLEDs, including the use of LiF/Al and Ca/Al as the cathode materials. Utilizing Mg-Ni nanoparticles to enhance electron injection and light-emitting characteristics of OLEDs appears to represent a practical approach to improving the overall device performance.

Acknowledgements This research has been supported by the US Department of Energy, Office of Energy Efficiency and Renewable Energy, under contract No. DE-AC02-05CH11231.

Open Access This article is distributed under the terms of the Creative Commons Attribution Noncommercial License which permits any noncommercial use, distribution, and reproduction in any medium, provided the original author(s) and source are credited.

References

1. C.W. Tang, S.A. Vanslyke, Appl. Phys. Lett. **51**, 913 (1987)
2. P.L. Burn, A.B. Holmes, A. Kraft, D.D.C. Bradley, A.R. Brown, R.H. Friend, R.W. Gymer, Nature **356**, 47 (1992)
3. J.H. Burroughs, D.D.C. Bradley, A.R. Brown, R.N. Marks, K. Mackay, R.H. Friend, P.L. Burn, A.B. Holmes, Nature **347**, 539 (1990)
4. M.A. Baldo, D.F. O'Brien, Y. You, A. Shoustikov, S. Sibley, M.E. Thompson, S.R. Forrest, Nature **395**, 151 (1998)
5. J.H. Choi, K.H. Kim, S.J. Choi, H.H. Lee, Nanotechnology **17**, 2246 (2006)
6. H.H.P. Gommans, M. Kemerink, G.G. Andersson, R.M.T. Pijper, Phys. Rev. B **69**, 155216 (2004)
7. D.K. Park, A.R. Chun, S.H. Kim, M.S. Kim, C.G. Kim, T.W. Kwon, S.J. Cho, H.S. Woo, J.G. Lee, S.H. Lee, Z.X. Guo, Appl. Phys. Lett. **91**, 052904 (2007)
8. I.D. Parker, J. Appl. Phys. **75**, 1656 (1994)
9. J.F. Wang, G.E. Jabbour, E.A. Mash, J. Anderson, Y. Zhang, P. Lee, N.R. Armstrong, N. Peygkambarian, Adv. Mater. **11**, 1266 (1999)
10. L.S. Hung, C.W. Tang, M.G. Mason, Appl. Phys. Lett. **70**, 152 (1997)
11. P. Piromerin, H. Oh, Y. Shen, G.G. Malliaras, J.C. Scott, P.J. Brock, Appl. Phys. Lett. **77**, 2403 (2000)
12. J. Birgerson, M. Fahlman, P. Broms, W.R. Salaneck, Synth. Met. **80**, 125 (1996)
13. D. Liu, M. Fina, Z. Chen, X. Chen, G. Liu, S. Johnson, S.S. Mao, Appl. Phys. Lett. **91**, 093514 (2007)
14. R.H. Flower, L. Nordheim, Proc. R. Soc. Lond., Ser. A **119**, 173 (1928)
15. S.M. Sze, *Physics of Semiconductor Devices* (Wiley, New York, 2007)